



Discovering the association between the pre- and post-operative 3D spinal curve patterns in adolescent idiopathic scoliosis

Saba Pasha¹ · Suken Shah² · Burt Yaszay³ · Peter Newton³ · Harms Study Group

Received: 20 September 2020 / Accepted: 14 December 2020 / Published online: 13 January 2021
© Scoliosis Research Society 2021

Abstract

Background The advantage of considering the three-dimensional curve patterns, including the patterns of the vertebral position and alignment, in classification of adolescent idiopathic scoliosis (AIS) patients and whether such classification system relates to the surgical outcomes are not fully determined.

Methods A total of 371 AIS patients who received posterior spinal fusion surgery with 2-year follow-up were included retrospectively and consecutively. The 3D positions and orientations of the T1–L5 vertebrae were calculated from the 3D reconstructions of the spines at pre-operative and 2-year follow-up, a total of 102 variables per patient. A probabilistic clustering method was used to cluster the pre-operative and 2-year follow-up 3D spinal curve patterns separately. The distributions of the Lenke types and 3D pre-operative clusters in the post-operative clusters were determined.

Results A total of nine pre-operative clusters including, four right thoracic types, three left thoracolumbar/lumbar types, one low apex right thoracic/thoracolumbar, and one left thoracic/right lumbar were determined. Three post-operative 3D curve patterns were Type 1 with higher residual proximal Cobb angle, Type 2 with lower T5–T12 kyphosis and highest pelvic incidence-lordosis mismatch, and Type 3 with larger lumbar curve magnitude and rotation compared to the other two groups. More than 50% of patients in each of the 3D pre-operative clusters had the same post-operative group.

Conclusion We developed a 3D classification of the AIS patients before and two-year after spinal fusion surgery. The link between the pre- and post-operative clusters lends itself to application of this classification system in developing predictive models of the AIS surgical outcomes.

Keywords Adolescent idiopathic scoliosis · 3D classification · Sagittal profile · Axial rotation · Surgical outcomes

Introduction

Variations in the two-dimensional (2D) and three-dimensional (3D) spinal curve patterns in adolescent idiopathic scoliosis (AIS) have been used to classify, guide clinical management of the patients, and predict treatment outcomes [1–4]. Several studies have determined surgical guidelines based on the King or Lenke classification [1, 2, 5–14]. Anecdotally adverse surgical outcomes have been observed

following these guidelines [13, 15–17]. A classification system that can differentiate between the key 3D curve characteristics and their association with the surgical outcomes is of critical need.

Lenke classification is currently the most common classification system for AIS [1]. This system uses the location (proximal thoracic, thoracic, or lumbar), number, and flexibility of the 2D frontal curves and adds sagittal and lumbar modifiers to determine the curve types [1]. Other studies considered the 3D parameters of the spine, particularly the axial rotation of the curves, and determined several subtypes within each Lenke type [18–20]. Classifications of the AIS based on the 3D vertebral positions have been developed [4, 18, 20–22]; however, the 3D alignment of the vertebral bodies in frontal, sagittal, and axial planes has not been included in the AIS classification. As the patient-specific vertebral relative alignments and disc wedging guide the surgical moves, it remains to

✉ Saba Pasha
pashas@pennmedicine.upenn.edu

¹ Department of Orthopedic Surgery, Perelman School of Medicine, University of Pennsylvania, Philadelphia, USA

² Department of Orthopedics, Nemours/Alfred I. duPont Hospital for Children, Wilmington, USA

³ Department of Orthopedic Surgery, Rady Children's Hospital, San Diego, USA

determine if considering the patterns of 3D alignments of the vertebral bodies at pre-operative, in addition to their 3D positions, can lead to a classification of AIS that is deterministic of the surgical outcomes. Moreover, the surgical outcome evaluation of AIS mainly focuses on one outcome at the time, while methods to assess the global alignment of the spine are not fully explored [9, 13, 21, 23].

To this end, we aimed to develop a classification system of the 3D spinal alignment before and at two-year follow-up of the posterior spinal fusion (PSF) using the 3D vertebral alignment and position. We further determined the distribution of the 3D pre-operative clusters in the 3D outcome groups. We hypothesized that a pre-operative classification of the spinal curve based on the 3D position and alignment of the vertebral bodies relates to the 3D global alignment of the spine at 2-year follow-up at a higher accuracy rate compared to the Lenke classification.

Methods

Patient population

AIS patients who had received a PSF with at least 2-year follow-up were reviewed in a multicenter (three) and multi-surgeon (seven) data registry. Patients with two-view (posterior–anterior and lateral) spinal stereoradiographs at pre-operative and 2-year follow-ups were included. Lenke type classification was extracted from the database. A total of 20 non-scoliotic adolescents were included.

Fig. 1 Vertebral 3D position (X, Y, Z) and 3D alignment parameters (Frontal and sagittal tilt and axial rotation). A vector constituted of these 6 variables was generated per vertebral level (17 vertebrae T1–L5). These variables were used in the classification algorithm. The origin of the coordinate system is the posterior aspect of the sacral plateau

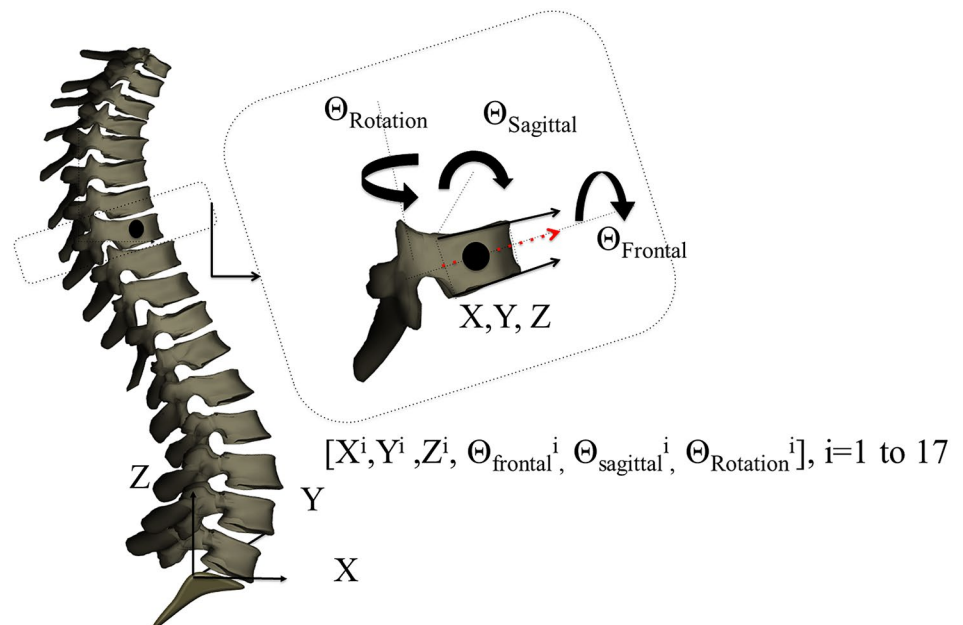


Image processing and variable extraction

3D reconstructions of the spine and pelvis radiographs were generated in SterEOS 2D/3D (EOS imaging, Paris, France) for pre- and post-operative images. Using the vertebral endplate alignments [24], the 3D model of the spine was used to measure the T1–T12 and T5–T12 kyphosis, L1–S1 lordosis, pelvic incidence (PI), proximal and main thoracic and lumbar coronal Cobb angles, and pelvic incidence. T1 to L5 vertebral 3D alignments, i.e., frontal tilt (Θ_{Frontal}), sagittal tilt (Θ_{Sagittal}), and axial rotation (Θ_{Rotation}), were calculated using the average of the vectors connecting the posterior and anterior points on the vertebral endplate on the superior and inferior endplates (Fig. 1) [25]. The angle between this average vector and the true X -, Y -, Z -axes determined the frontal, sagittal, and axial alignment of the vertebrae (Fig. 1). The vertebral centroids were calculated using the 3D reconstruction models [25]. The image analysis extracted a total of 6 variables per vertebra, 102 variables per spine (Fig. 1). The X -, Y -, Z -coordinates were scaled isotropically in a way to achieve normalized height [4, 20]. The vertebral 3D alignments were standardized (divided by standard deviation and the mean was removed) to eliminate the effect of the severity of the curve, which allowed performing the classification based on the deformity patterns, solely.

Clustering analysis

The 102 variables per patient were used to determine the pre- and postoperative 3D clusters. A fuzzy C-means clustering with 1000 non-repetitive start points was used

to calculate the degree of membership of patients to each cluster. The maximum degree of membership determined the cluster number. The cluster analysis was performed for pre- and post-operative spines separately.

Each cluster was described based on the curve pattern characteristics in three anatomical planes. Hypo ($< 10^\circ$), hyper- ($> 40^\circ$), and normal kyphosis (between 10° and 40°) were defined according to Lenke classification [1]. In each cluster, the axial projection was presented based on a previous classification of the curves projection on the transverse plane [20, 26]: in the loop shaped axial projection, the vertebral rotation outside of the main curve does not change; thus, the vertebrae are rotated in the same direction or not rotated at all. In the lemniscate type, the direction of the vertebral rotation is different between the main and compensatory curves resulting in thoracic and lumbar vertebrae rotated into opposite directions projecting a lemniscate shape on the axial plane.

Statistical analysis

The spinal and pelvic measurements in each of the pre- and post-operative clusters were statistically compared. The distributions of the pre-operative clusters in the Lenke types and in the 3D outcome clusters were determined.

Results

A total of 371 AIS patients were included. All Lenke types were included: Lenke 1 (35%), Lenke 2 (23%), Lenke 3 (10%), Lenke 4 (7%), Lenke 5 (15%), and Lenke 6 (10%). The clustering analysis determined nine pre-operative 3D clusters.

Pre-operative clusters

Table 1 summarizes the spinal and pelvic measurements in the pre-operative clusters. Analysis of variance for each variable showed significant differences between the clusters (Table 1). Figure 2 shows the frontal, lateral, and axial views of the preoperative clusters.

The nine pre-operative group description in 3D, frontal plane, sagittal plane, and axial plane are as follows:

(A) Patients appear with a right thoracic curve, which exceeds the left lumbar Cobb angle in frontal plane; includes Type 1 to Type 4 curve patterns. 65% of the patients belonged in this group.

Type 1—two 3D curves. Hyperkyphotic. The axial projection is lemniscate shaped.

Type 2—one 3D curve. Kyphosis was in the hypokyphotic–normal range, long frontal thoracic curve with small

or no rotation in lumbar spine. Highest pelvic incidence among the subtypes. The axial projection is loop shaped.

Type 3—two 3D curves. Thoracic and lumbar curves are close in magnitude. Normal kyphosis. The axial projection is lemniscate shaped.

Type 4—one 3D curve. Hypokyphotic with long lordotic curve. The axial projection is loop shaped.

(B) Patients with a left lumbar curve, which exceeds the right thoracic Cobb angle; includes Type 5 to Type 7 curve patterns. 27% of the patients belonged in this group.

Type 5—one 3D curves. Hyper to Normal kyphosis. Long kyphotic curve. The axial projection is loop shaped.

Type 6—two–three 3D curves. Normal to Hypokyphosis. The axial projection is lemniscate shaped.

Type 7—two–three 3D curves. Hypokyphotic. Flat T4–T12 kyphosis. Lowest pelvic incidence. The axial projection is lemniscate shaped.

(C) Type 8—low apex right thoracic curve. One 3D curves. The apex of the thoracic curve is lower than the subtypes in section A (right thoracic curves). Normal–hyper kyphosis. The axial projection is loop shaped.

(D) Type 9—left thoracic/right lumbar. One 3D curve—Hyperlordotic. Long lordotic curve. The axial projection is loop shaped.

The distribution of the Lenke types in each of the 3D pre-operative clusters is shown in Table 2. These most common Lenke types comprised at least 25% of the patients in each of 3D clusters (Table 2).

Post-operative clusters

Three post-operative 3D clusters were determined based on our clustering analysis with a distribution of Type 1 (41%), Type 2 (35%), and Type 3 (24%) (Fig. 3). The average frontal, sagittal, and axial spinal and pelvic parameters in each outcome subtypes are presented in Table 3. Type 1 and type 2 had similar frontal profile while Types 1 and 3 had similar sagittal profile (Fig. 3 and Table 3). Type 1 had the highest proximal thoracic Cobb angle and lowest PI and Type 3 had the lowest proximal thoracic Cobb and the highest lumbar Cobb angle and rotation, $p < 0.05$ (Table 3). Type 2 had the lowest T5–T12 kyphosis and pelvic incidence–lordosis mismatch (PI-LL) compared to the other two types, $p < 0.05$ (Table 3).

Link between the pre-operative cluster (3D and Lenke) and post-operative 3D clusters

A majority (50% and higher) of the patients in the pre-operative 3D types 1, 3, 4, 8, and 9 had the Type 1 outcome profiles (Table 4). 68% of pre-operative cluster Type 2 had the Type 2 outcomes. More than 50% in Types 5, 6, 7 had type 3 outcomes (Table 4).

Table 1 The spinal and pelvic measurements in the preoperative subtypes

3D clusters	PT	PT apical rotation	MT	MT apical rotation	TL/L	L apical rotation	T1–T12 kyphosis	T5–T12 kyphosis	L1–S1 lordosis	PI
1 n=39	30.2±9.7*	9.5±4.9	61.4±12.1*	-21.3±7.9*	38.3±9.6	8.6±4.7	51.2±10.8*	40.1±10.8*	62.3±11.6*	45.7±11.9
2 n=44	30.1±9.1*	9.0±5.6	57.3±9.5	-20.3±7.2*	33.7±9.1*	4.5±5.3*	35.5±9.9	23.2±8.1*	63.5±8.6*	58.2±10.6*
3 n=86	24.4±7.2	9.6±4.7	56.2±10.8	-13.9±5.7	42.9±9.3	12.2±4.6	29.3±9.2*	19.6±10.3*	56.9±10.0	53.7±12.5
4 n=72	29.3±8.4*	11.0±5.0*	53.5±9.7	-16.8±5.9	30.7±10.5*	3.6±6.0*	14.3±9.2*	4.6±8.8*	46.3±9.6*	49.3±11.6
5 n=48	11.2±7.5*	3.7±3.4*	31.4±10.9*	1.3±8.5*	42.5±11.6	19.7±9.4	36.1±9.9	28.0±8.6	56.6±10.2	47.9±10.5
6 n=10	9.8±6.1*	10.4±3.9	47.1±11.2	-2.1±5.0	60.5±9.0*	31.0±4.5*	20.9±9.8*	20.3±9.6*	41.2±10.3*	36.7±8.0*
7 n=43	18.1±7.9	11.3±5.1*	55.5±17.3	-8.1±7.2	58.2±13.9*	24.6±8.1	18.0±10.4*	10.1±9.1*	52.6±10.8	54.9±9.4
8 n=17	24.0±16.3	4.9±5.9	48.6±23.4	-16.3±11.3	33.4±21.4*	-10.7±14.4*	38.5±13.0	30.5±11.1	59.2±11.4	42.2±8.9
9 n=12	13.9±9.1*	-5.9±5.3*	42.2±12.6	5.0±9.4*	43.1±11.5	-17.1±10.8*	24.1±12.1*	20.7±10.1*	56.7±15.9	51.5±16.1
p value	0.033	0.041	0.038	0.031	0.036	0.022	0.024	0.030	0.038	0.041

Significantly different variables at $\alpha=0.05$ between the types are shown by asterisk

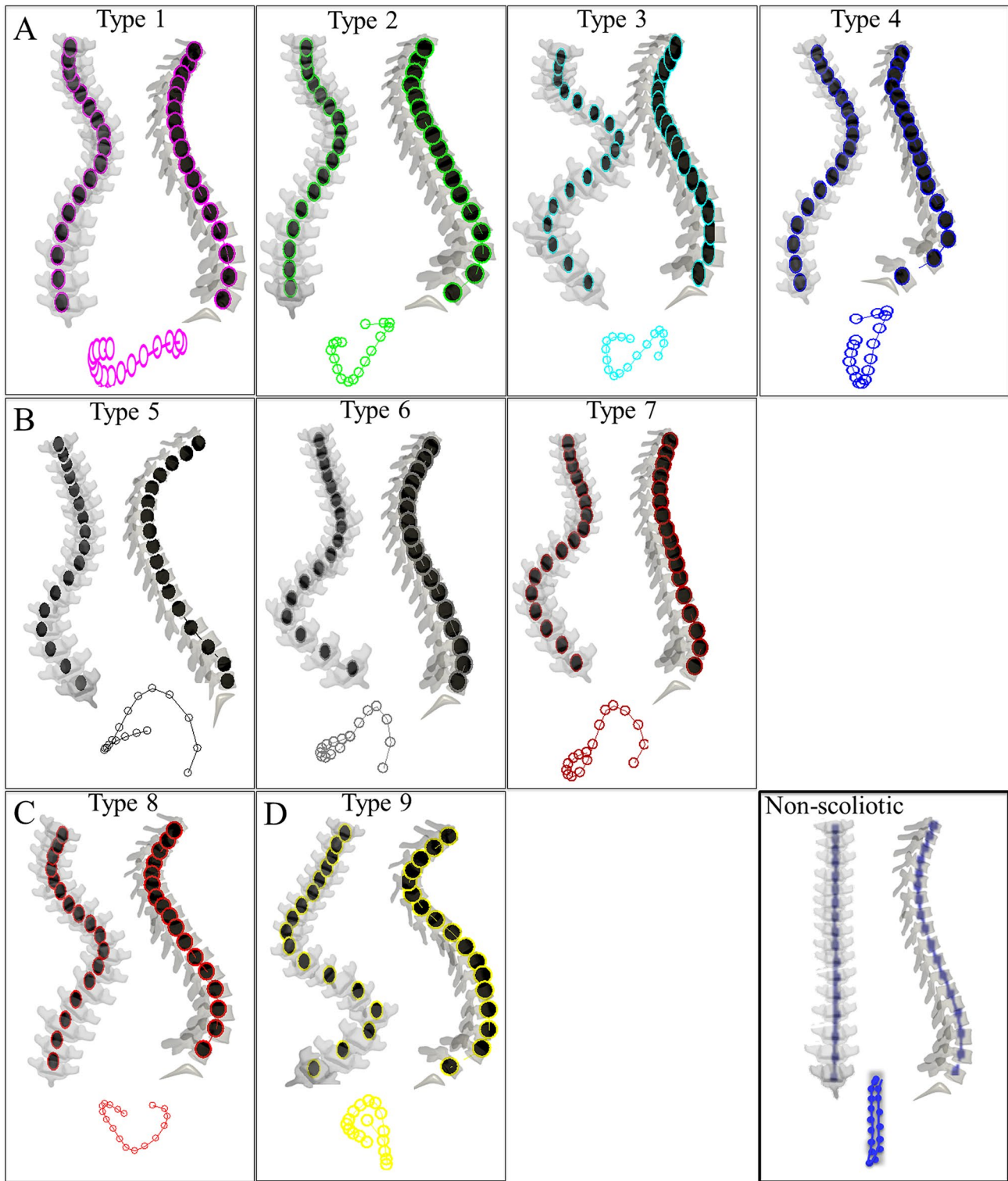


Fig. 2 Pre-operative clusters of the AIS cohort. A total of nine 3D curve patterns were identified. **a** Types 1–4: right thoracic curves. **b** Types 5–7 left thoracolumbar/lumbar curves. **c** Type 8: right low apex thoracic/thoracolumbar and **d** Type 9: left thoracic right lumbar

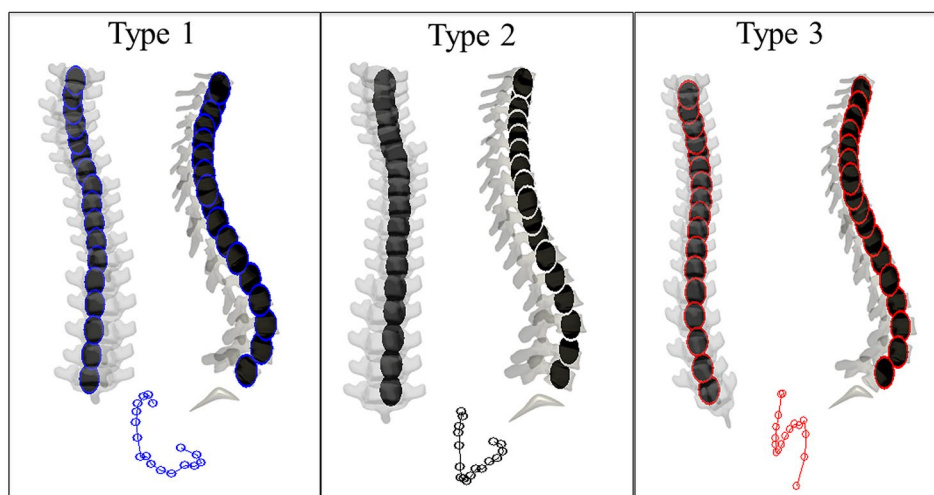
curve. Summary of the spinal parameters for each cluster is listed in Table 1. The average spinal alignment in the cohort of 20 non-scoliotic adolescents is included

Table 2 Distribution of the nine preoperative 3D clusters based on the Lenke criteria

3D clusters	Lenke type						Lumbar modifier			Kyphosis modifier		
	1	2	3	4	5	6	A	B	C	–	N	+
1	35	29	18	18	–	–	44	48	8	–	40	60
2	33	46	9	11	–	–	86	11	2	7	86	7
3	58	16	17	6	1	2	23	34	44	11	81	8
4	51	44	2	3	–	–	87	11	1	69	31	–
5	6	–	–	4	73	17	–	–	100	4	82	14
6	–	–	–	–	30	70	–	–	100	10	90	–
7	12	2	14	16	14	42	–	–	100	65	35	–
8	35	24	–	6	20	16	59	6	35	6	77	18
9	27	10	18	0	35	10	40	–	60	–	90	10

The number are presented in percent (%)

Fig. 3 Post-operative clusters of the cohort. A total of three 3D curve patterns were identified. Residual proximal thoracic in Type 1, hypokyphosis in Type 2, and residual lumbar Cobb angle and rotation in Type 3 were the main characteristics. Summary of the spinal parameters for each cluster are listed in Table 3



Considering the distribution of the Lenke types in the outcome groups, more than 50% of the Lenke Types 2, 5 and 6 ended up in one outcome group (Table 5) while the relationship between Lenke 1, 3, and 4 and the outcome clusters was inconclusive (Table 5).

Discussion

A 3D classification system that distinguishes between the pre-operative curve patterns and associates pre-operative curve types with the post-operative global spinal alignment is the first step in developing data-driven models for PSF outcome prediction. We developed a classification system based on the 3D curve patterns of the AIS patients before and two years after surgery. Considering these patterns, we discovered strong associations between the spinal alignment at pre-operative and 2-year follow-ups.

Classifications of the spinal deformity in AIS are mainly based on 2D radiographs [1, 2]. Lenke classification uses 6 frontal curve patterns, three kyphosis modifiers, and

three lumbar modifiers [1]. Eliminating the non-plausible combinations (Lenke 5A and 6A for example), approximately 45 different combinations of the Lenke types with modifiers can be determined. Our analysis showed a total of nine 3D subtypes, each composed of several Lenke types (Fig. 2; Table 2). While we determined the dominant Lenke type within each of these 3D clusters, the percent of patients with the same Lenke type in the 3D clusters remained low and exceeded 50% in only two subtypes (Table 2). Our classification specially draws attention to variation in the axial and sagittal curvature of the spine in patients with thoracic or thoracolumbar curves (Fig. 2). The axial patterns determined the number of 3D curves in loop versus lemniscate shaped axial projection types (Fig. 2). The sagittal curves of the subtypes showed a high variation in the position of the inflection point, a factor that was not accessible in the Lenke classification which can better guide the selection of the fusion levels and imparting kyphosis/lordosis. Our results showed considering the 3D clusters can determine different curve patterns within the Lenke types, which in turn can facilitate

Table 3 The spinal and pelvic measurements in the subtypes at 2-year follow-up

Post-op cluster	PT	PT apical rotation	MT	MT apical rotation	TL/L	L apical rotation	T1–T12 kyphosis	T5–T12 kyphosis	L1–S1 lordosis	PI
1	15.3±5.0*	2.6±5.3	16.1±8.5	-7.1±6.7*	12.9±7.7*	5.5±7.7*	38.0±8.9	28.5±9.9*	52.2±9.7	44.7±9.1*
2	13.8±7.7	3.1±4.6	15.8±7.8	-4.9±6.5*	11.2±7.0*	3.0±6.6*	36.0±8.8	17.6±9.8*	65.8±10.0	66.5±12.3*
3	9.8±6.6*	6.7±4.7	21.2±12.0	4.0±6.4*	23.9±7.3*	15.2±7.4*	36.5±9.1	25.9±11.0	62.0±8.9	57.3±14.0
<i>p</i> value	0.046	NS	NS	0.036	0.033	0.027	NS	0.033	NS	0.036

Significantly different variables at $\alpha=05$ between the types are shown by asterisk

NS non-significant

communicating these differences between the surgeons. It should be kept in mind that variations between the individuals, scoliotic and non-scoliotic alike, within a cluster is expected (Fig. 2).

The role of the 3D descriptors of the scoliotic curves, particularly the axial rotations, has been underlined in the literature [18–20, 24, 27]. Despite the increased use of stereoradiography in orthopedic clinics, the application of the 3D models of the spine in clinical diagnostics remains limited. Vertebral rotation [18], orientation of the plane of maximum curvature [18, 28], global torsion [22] and writhe [29] of the spinal centerline were used to identified subtypes of AIS patients. All these methods, although determined fundamental differences between the curve patterns within the AIS types, required intensive image post processing and analysis[29]. Our classification uses the 3D position and alignment of the vertebral bodies to determine the 3D clusters, but subsequently describes the curve patterns in the frontal, sagittal, axial characteristics (loop, lemniscate) using 2D radiographs of the spine (Fig. 2). A classification system that relies on a few curve patterns reduces the need to excessive image processing and can facilitate the clinical application of this classification.

In the current analysis, we determined two distinct axial projection patterns of the curves in our cohort of all Lenke types (Fig. 2). These patterns, i.e., loop versus lemniscate axial projections were also observed in previous classifications of the scoliosis [16, 20, 26] and determined the number of true 3D curves [20, 26]. In group A (Types 1–4) and group B (Types 5–7) two 3D curves was observed in Types 1, 3, 6, 7 (lemniscate axial projection), while in the types with loop shaped axial projection (Types 2, 4, 5) the vertebral rotation in the secondary curve are insignificant showing only one 3D curve. It was shown before that a correct identification of these 3D curves extents can impact the outcomes of the PSF [16]. It was shown when a 3D curve was included in the fusion While the measurements of the vertebral axial rotation on 2D radiographs is less reliable [30], the patterns of changes in the pedicle orientations can be detected with high accuracy ($\kappa=0.98$) using only the 2D radiographs and can be used to determine the AIS subtypes [31]. The low apex thoracic curve patients (Type 8) show essentially different curve patterns when compared with groups A and B clusters, as was also suggested before [32]. Our analysis separated this cohort (Type 8) from thoracic curve groups (Types 1–4) showing that although Type 8 has a similar axial pattern to Types 2 and 4 but the sagittal and frontal curves do not match any of these curve patterns revealing differences between the low apex thoracic and typical thoracic and thoracolumbar curves (Fig. 2). Type 9 not only had a left thoracic curve but also the sagittal and axial curves were different from the other thoracic types suggesting a significantly different 3D curve pattern (Fig. 2).

Table 4 Proportion of the 3D preoperative clusters in the three outcome clusters

Preop	1	2	3	4	5	6	7	8	9
Postop									
1	72	30	50	56	15	30	9	65	50
2	18	68	31	42	17	0	35	29	50
3	10	2	19	1	69	70	56	6	0

Table 5 Proportion of the Lenke types in the three outcome clusters

Preop	Lenke 1	Lenke 2	Lenke 3	Lenke 4	Lenke 5	Lenke 6
Postop						
1	47	58	46	24	22	13
2	42	40	22	45	20	31
3	12	2	32	31	59	56

Instead of focusing on one radiographic outcome, we clustered the 3D spinal alignment at 2-year follow-ups to determine significantly different global spinal alignments as our surgical outcome measure (Fig. 3). While the preoperative 3D clusters related to the outcome curve patterns (Table 4), the role of the surgical factors in achieving specific outcomes cannot be ignored [21]. In the current cohort, while variation in the surgical technique existed between the surgeons, a majority of the patients received the same treatment [33]. These surgical moves/techniques included: intraoperative traction, rod tensile strength (200 KSI both rods), all screws construct type, in situ bending, Ponte Osteotomy, wide posterior release, segmental derotation with two rods in, and both ends locked before direct vertebral rotation. Identifying the surgical parameters, specific to each of the 3D pre-operative clusters, can increase the likelihood of achieving one of the outcome types. This is the subject of our future study.

A previous 3D classification of all Lenke types used 2D measurements of the spine and the plane of maximum curvature as variables and determined 11 subtypes of scoliosis [28]. The subtypes were characterized as low, average, and high for frontal curves and hypo, hyper, neutral for sagittal curves. As a result, this classification determined subtypes by relying on curve magnitudes [28]. Our classification, however, used the patterns of the normalized values of the vertebral position and alignment thus eliminating the effect of the curve severity in our classification while allowed identifying different curve patterns (Table 1; Figs. 2 and 3). As seen in Table 1, the variations in the pre-operative frontal curve magnitudes in our classification were smaller than the previous 3D classification system [28].

The relationship between the pre- and post-operative clusters remains to be tested for a verity of surgical techniques to better evaluate reproducibility and reliability of the proposed classification system. External validations of the method to

verify if these curve patterns can be learned and used by orthopedic surgeons are warranted.

Conclusion

A new AIS classification of the pre- and post-operative spinal 3D curve patterns was developed. We discovered a relationship between the pre-operative clusters and the post-operative groups, showing the clinical relevance of this classification and a promising application of this classification in PSF outcome prediction.

Author contributions SP, SS, BY, and PN: made substantial contributions to the conception or design of the work; or the acquisition, analysis, or interpretation of data; or the creation of new software used in the work; SP, SS, BY, and PN: drafted the work or revised it critically for important intellectual content; SP, SS, BY, and PN: approved the version to be published; SP, SS, BY, and PN: agree to be accountable for all aspects of the work in ensuring that questions related to the accuracy or integrity of any part of the work are appropriately investigated and resolved.

Funding This study was funded by Scoliosis Research Society and National Institute of Health in form of grant to SP (1R21AR075971-01A1).

Compliance with ethical standards

Conflict of interest SP (grants from NIH and SRS), BY (grants and personal fees from K2M, DePuy Synthes Spine, and NuVasive; personal fees from Medtronic, Orthopediatrics, Stryker, Globus, and Biogen; grants from Setting Scoliosis Straight Foundation, outside the submitted work; in addition, BY has a patent K2M with royalties paid), PON (other from DePuy Synthes, K2M, OrthoPediatrics, NuVasive, and AlphaTec, during the conduct of the study; grants and other from Setting Scoliosis Straight Foundation; other from Rady Children's Specialists; grants, personal fees, and nonfinancial support from DePuy Synthes Spine and K2M; grants and other from SRS; grants from EOS Imaging; personal fees from Thieme Publishing; grants from Nu-

Vasive; other from Electrocore; personal fees from Cubist; other from International Pediatric Orthopedic Think Tank; grants, nonfinancial support, and other from Orthopediatrics; grants and nonfinancial support from Alphatech; grants from Mazor Robotics, outside the submitted work; in addition, PON has a patent “Anchoring Systems and Methods for Correcting Spinal Deformities” [8540754] with royalties paid to DePuy Synthes Spine; a patent “Low Profile Spinal Tethering Systems” [8123749] licensed to DePuy Spine, Inc.; a patent “Screw Placement Guide” [7981117] licensed to DePuy Spine, Inc.; a patent “Compressor for Use in Minimally Invasive Surgery” [7189244] licensed to DePuy Spine, Inc.; and a patent “Posterior Spinal Fixation” pending to K2M).

Research involving human participants and/or animals All procedures performed in studies involving human participants were in accordance with the ethical standards of the institutional and/or national research committee and with the 1964 Helsinki declaration and its later amendments or comparable ethical standards.

Informed consent Informed consent was obtained from all individual participants included in the study.

References

1. Lenke LG, Betz RR, Harms J, Bridwell KH, Clements DH, Lowe TG, Blanke K (2001) Adolescent idiopathic scoliosis: a new classification to determine extent of spinal arthrodesis. *J Bone Joint Surg Am* 83:1169–1181
2. King HA, Moe JH, Bradford DS, Winter RB (1983) The selection of fusion levels in thoracic idiopathic scoliosis. *J Bone Joint Surg Am* 65:1302–1313
3. Pasha S (2019) 3D spinal and rib cage predictors of brace effectiveness in adolescent idiopathic scoliosis. *BMC Musculoskelet Disord* 20:384. <https://doi.org/10.1186/s12891-019-2754-2>
4. Duong L, Mac-Thiong JM, Cheriet F, Labelle H (2009) Three-dimensional subclassification of Lenke type 1 scoliotic curves. *J Spinal Disord Tech* 22:135–143. <https://doi.org/10.1097/BSD.0b013e31816845bc>
5. Ferrero E, Bocahut N, Lefevre Y, Roussouly P, Pesenti S, Lakhali W, Odent T, Morin C, Clement JL, Compagnon R, de Gauzy JS, Jouve JL, Mazda K, Abelin-Genevois K, Ilharreborde B, (GES) GdEsIS (2018) Proximal junctional kyphosis in thoracic adolescent idiopathic scoliosis: risk factors and compensatory mechanisms in a multicenter national cohort. *Eur Spine J* 27:2241–2250. <https://doi.org/10.1007/s00586-018-5640-y>
6. Pasha S, Mac-Thiong JM (2019) Defining criteria for optimal lumbar curve correction following the selective thoracic fusion surgery in Lenke 1 adolescent idiopathic scoliosis: developing a decision tree. *Eur J Orthop Surg Traumatol*. <https://doi.org/10.1007/s00590-019-02596-z>
7. Qin X, He Z, Yin R, Qiu Y, Zhu Z (2020) Selecting the last substantially touching vertebra as lowest instrumented vertebra in Lenke type 2A-R and 2A-L curves. *Spine (Phila Pa 1976)* 45:309–318. <https://doi.org/10.1097/BRS.0000000000003254>
8. Skaggs DL, Seehausen DA, Yamaguchi KT, Hah RJ, Wright ML, Bumpass DB, Kim HJ, Andras LM, Vitale MG, Lenke LG (2016) Assessment of lowest instrumented vertebra tilt on radiographic measurements in Lenke “C” modifier curves undergoing selective thoracic fusion in adolescent idiopathic scoliosis. *Spine Deform* 4:125–130. <https://doi.org/10.1016/j.jspd.2015.08.006>
9. Lonner BS, Ren Y, Newton PO, Shah SA, Samdani AF, Shuffelbarger HL, Asghar J, Sponseller P, Betz RR, Yaszay B (2017) Risk factors of proximal junctional kyphosis in adolescent idiopathic scoliosis—the pelvis and other considerations. *Spine Deform* 5:181–188. <https://doi.org/10.1016/j.jspd.2016.10.003>
10. Crawford CH, Lenke LG, Sucato DJ, Richards BS, Emans JB, Vitale MG, Erickson MA, Sanders JO (2013) Selective thoracic fusion in Lenke 1C curves: prevalence and criteria. *Spine (Phila Pa 1976)* 38:1380–1385. <https://doi.org/10.1097/BRS.0b013e3182987360>
11. Lenke LG, Betz RR, Haheer TR, Lapp MA, Merola AA, Harms J, Shuffelbarger HL (2001) Multisurgeon assessment of surgical decision-making in adolescent idiopathic scoliosis: curve classification, operative approach, and fusion levels. *Spine (Phila Pa 1976)* 26:2347–2353
12. Homans JF, Kruyt MC, Schlösser TPC, Colo D, Rogers K, Shah SA, Flynn JM, Castelein RM, Pasha S (2020) Changes in the position of the junctional vertebrae after posterior spinal fusion in adolescent idiopathic scoliosis: implication in risk assessment of proximal junctional kyphosis development. *J Pediatr Orthop* 40:e84–e90. <https://doi.org/10.1097/BPO.0000000000001400>
13. Schulz J, Asghar J, Bastrom T, Shuffelbarger H, Newton PO, Sturm P, Betz RR, Samdani AF, Yaszay B, Group HS (2014) Optimal radiographical criteria after selective thoracic fusion for patients with adolescent idiopathic scoliosis with a C lumbar modifier: does adherence to current guidelines predict success? *Spine (Phila Pa 1976)* 39:E1368–1373. <https://doi.org/10.1097/BRS.0000000000000580>
14. Pasha S, Cahill PJ, Flynn JM, Sponseller P, Newton PO, Group aHS (2018) Relationships between the axial derotation of the lower instrumented vertebra and uninstrumented lumbar curve correction: radiographic outcome in Lenke 1 adolescent idiopathic scoliosis with a minimum 2-year follow-up. *J Pediatr Orthop* 38:e194–e201. <https://doi.org/10.1097/BPO.0000000000001136>
15. Chang KW, Leng X, Zhao W, Chen YY, Chen TC, Chang KI (2011) Broader curve criteria for selective thoracic fusion. *Spine (Phila Pa 1976)* 36:1658–1664. <https://doi.org/10.1097/BRS.0b013e318215fa73>
16. Pasha S, Baldwin K (2019) Surgical outcome differences between the 3D subtypes of right thoracic adolescent idiopathic scoliosis. *Eur Spine J*. <https://doi.org/10.1007/s00586-019-06145-4>
17. Cho RH, Yaszay B, Bartley CE, Bastrom TP, Newton PO (2012) Which Lenke 1A curves are at the greatest risk for adding-on... and why? *Spine (Phila Pa 1976)* 37:1384–1390. <https://doi.org/10.1097/BRS.0b013e31824bac7a>
18. Sangole AP, Aubin CE, Labelle H, Stokes IA, Lenke LG, Jackson R, Newton P (2009) Three-dimensional classification of thoracic scoliotic curves. *Spine (Phila Pa 1976)* 34:91–99. <https://doi.org/10.1097/BRS.0b013e3181877bbb>
19. Shen J, Kadoury S, Labelle H, Parent S (2016) Geometric torsion in adolescent idiopathic scoliosis: a surgical outcomes study of Lenke type 1 patients. *Spine (Phila Pa 1976)* 41:1903–1907. <https://doi.org/10.1097/BRS.0000000000001651>
20. Pasha S, Hassanzadeh P, Ecker M, Ho V (2019) A hierarchical classification of adolescent idiopathic scoliosis: identifying the distinguishing features in 3D spinal deformities. *PLoS ONE* 14:e0213406. <https://doi.org/10.1371/journal.pone.0213406>
21. Pasha S, Flynn J (2018) Data-driven classification of the 3D spinal curve in adolescent idiopathic scoliosis with an applications in surgical outcome prediction. *Sci Rep* 8:16296. <https://doi.org/10.1038/s41598-018-34261-6>
22. Kadoury S, Shen J, Parent S (2014) Global geometric torsion estimation in adolescent idiopathic scoliosis. *Med Biol Eng Comput* 52:309–319. <https://doi.org/10.1007/s11517-013-1132-8>
23. Louer C, Yaszay B, Cross M, Bartley CE, Bastrom TP, Shah SA, Lonner B, Cahill PJ, Samdani A, Upasani VV, Newton PO (2019) Ten-year outcomes of selective fusions for adolescent idiopathic scoliosis. *J Bone Joint Surg Am* 101:761–770. <https://doi.org/10.2106/JBJS.18.01013>

24. Pasha S, Cahill PJ, Dormans JP, Flynn JM (2016) Characterizing the differences between the 2D and 3D measurements of spine in adolescent idiopathic scoliosis. *Eur Spine J* 25:3137–3145. <https://doi.org/10.1007/s00586-016-4582-5>
25. Pasha S, Schlösser T, Zhu X, Castelein R, Flynn J (2019) Application of low-dose stereoradiography in in vivo vertebral morphologic measurements: comparison with computed tomography. *J Pediatr Orthop* 39:487–494. <https://doi.org/10.1097/BPO.0000000000001043>
26. Pasha S (2019) 3D deformation patterns of s shaped elastic rods as a pathogenesis model for spinal deformity in adolescent idiopathic scoliosis. *Sci Rep* 9:1
27. Stokes IA, Sangole AP, Aubin CE (2009) Classification of scoliosis deformity three-dimensional spinal shape by cluster analysis. *Spine (Phila Pa 1976)* 34:584–590. <https://doi.org/10.1097/BRS.0b013e318190b914>
28. Shen J, Parent S, Wu J, Aubin C, Mac-Thiong JM, Kadoury S, Newton P, Lenke LG, Lafage V, Barchi S, Labelle H (2020) Towards a new 3D classification for adolescent idiopathic scoliosis. *Spine Deform*. <https://doi.org/10.1007/s43390-020-00051-2>
29. Arginteanu T, DeTurck D, Pasha S (2020) Application of Călugăreanu–white–fuller theorem in classification of pediatric spinal deformity. *Med Biol Eng Comput* 58:2963
30. DeFrancesco CJ, Pasha S, Miller DJ, Betz RR, Clements DH, Fletcher ND, Glotzbecker MG, Hwang SW, Kelly MP, Lehman RA, Lonner BS, Newton PO, Roye BD, Sponseller PD, Upasani VV, Cahill PJ, Group HS (2018) Agreement between manual and computerized designation of neutral vertebra in idiopathic scoliosis. *Spine Deform* 6:644–650. <https://doi.org/10.1016/j.jspd.2018.03.001>
31. Pasha S, Ho-Fung V, Ecker M, Nossov S, Francavilla M (2020) Three-dimensional classification of the Lenke 1 adolescent idiopathic scoliosis using coronal and lateral spinal radiographs: a validation study. *BMC Musculoskelet Disord* 21:1
32. Alam M, Newton PO, Yaszay B, Bastrom TP, Group HS (2013) Are thoracic curves with a low apex (T11 or T11/T12) really thoracic curves? *Spine Deform* 1:139–143. <https://doi.org/10.1016/j.jspd.2012.12.004>
33. Pasha S, Shah S, Newton P (2020) Machine learning predicts the 3D outcomes of adolescent idiopathic scoliosis surgery using patient-surgeon specific parameters. *Spine*. <https://doi.org/10.1097/BRS.0000000000003795>

Publisher's Note Springer Nature remains neutral with regard to jurisdictional claims in published maps and institutional affiliations.